International Journal of Thin Films Science and Technology

http://dx.doi.org/10.12785/ijtfst/030103

Effect of Thickness and Annealing on Structural and Optical Properties of Bi2Te3 Thin Films Prepared from Bi2Te3 Nanoparticels

S. M. Elahi[1,*], *A. Taghizadeh*[2], *A. Hadizadeh*[2] *and L. Dejam*[1]

[1] Plasma research center, Science and research Branch Islamic Azad University, Tehran, Iran
[2] Department of Physics, Faculty of Science, University of Razi, Kermanshah, Iran

Received: 7 Jun. 2013, Revised: 21 Sep. 2013, Accepted: 23 Sep. 2013
Published online: 1 Jan. 2014

Abstract: Thin films Bi2Te3 with the thickness range of 37-110 nm have been deposited on clean glass substrates by the thermally evaporated technique in a vacuum of 1 10 -5 Torr. The influence of thickness and annealing on the structural and optical properties has been studied. The XRD patterns showed after thermal annealing the Bi2Te3 thin films became polycrystalline in structure. The lattice parameters of the samples were calculated and the structural parameters were discussed on the basis of annealing effect. The AFM images revealed a homogeneous Bi2Te3 dispersion within the layer in higher annealing temperature. Absorption spectra indicate that films were having considerable absorption throughout visible region. Optical band gap energy decreased with increasing film thickness and annealing temperature.

Keywords: Bismuth Telluride,Thin films,X-ray diffraction,AFM,Band gap energy

1 Introduction

The V-VI binary compounds such as Bi2S3, Bi2Te3 and Bi2Se3 are narrow band gap semiconductors with homologous layered crystal which are becoming quite interesting and important [1,2,3,4]. because of major contribution in solar cells, photo detectors, opto-electronic, light amplifiers, electro-photography, light emitting diodes, lasers and photo electrochemical cells. The best materials for thermoelectric applications are narrow band gap semiconductors with layered structure. Bi2Te3 thin films have been studied for applications to the effective sensing and controlling of temperature at localized areas such as microelectronic devices [5,6]. Many studies have been made in recent years to improve the thermoelectric properties of Bi2Te3 [7,8,9,10].It is a common practice to fabricate Bi2Te3-based thermoelectric materials by single crystal growth[11,12] , sintering [13] , mechanical alloying [14, 15,16], hot pressing [17] , hot extrusion [18] , electrochemical atomic layer epitaxy [19,**?**], etc. In our knowledge, there is no report on thermal evaporated Bi2Te3 thin films that prepared from Bi2Te3 nano-particle. In this work the nano-particles are made by sonochemical method and we report detailed study of the influence of thickness and annealing temperatures on structural and optical properties of thermal evaporated Bi2Te3 thin films of Bi2Te3 nano-particles.

2 Experimental setup

Bismuth telluride thin films were deposited onto ultrasonically cleaned glass substrates with a rectangular shape of 1625 mm at room temperature. The powder Bi2Te3 nano-particles was made by Sonochemical method. The Bicl3 and Te powders were used as 2:3 molar ratio reactant in presence of double-distillated water as solvent. NaBH4 was utilized as reductive and NaoH for alcolinization of the medium. The solution has placed into ultrasonic system, with 23 kHz frequency and 70 C water for four hours. A thin molybdenum boat was used for evaporation and it was heated by the Joule effect at a vacuum of 10-5 Torr. The sample with thickness of 70 nm was annealed at 400,420,435 and 450 K for 1 h.

* Corresponding author e-mail: smohammad_elahi@srbiau.ac.ir

3 Characterization

Structural analysis was performed for samples with 70 nm thickness before and after annealing using Philip Analytical X-ray difractometer, with the filtered CuKα radiation of wavelength 1.5418 A^o. The film surface morphology was analyzed by atomic force microscopy (AFM); model Park scientific, in contact mode. Also, the AFM investigation was utilized to determine the roughness of the surface films. Optical investigations in the visible range were performed using a spectrometer (UV-Visible AGILEN 8453) which allows measurement in the spectral range of 200-1000 nm. The transmittance measurements were used to calculate the absorption coefficient and optical band gap energies.

Table 1: Structural parameter of as-grown and annealed Bi2Te3 thin films of 70 nm

Thickness (nm)	Annealing Temp. °K	Grain size (nm)	Strain 10^{-3}	Dislocation density (cm^{-2}) 10^{12}
70	.....	11.66	2.94	0.94
	400	14.08	2.43	0.64
	420	15.83	2.16	0.51
	435	16.36	2.09	0.47
	450	21.79	1.68	0.31

Table 2: The morphology parameters of the films

Thickness (nm)	Anneal. Temp (°K)	Rp-v Å	Rms rough Å	Averough Å	Mean Ht Å
37	.....	145	112	8.06	59.2
110	.....	141	145	10.6	54.8
70	400	39.2	3.86	2.74	18.9
	450	47.8	5.85	4.38	22.7

Table 3: Variation of Abs. coefficient vs. thickness in Wavelenght=400 nm

Thickness (nm)	Abs. number	Abs. coeff (cm^{-1})
58	0.005679	0.98×10^3
70	0.014769	2.12×10^3
84	0.055890	6.84×10^3
110	0.534465	69.50×10^3

4 Results and discussion

4.1 XRD studies

X-ray diffraction studies were made on powder and thin films deposited on glass substrates to determine their structural parameters. X-ray diffraction patterns of the Bi2Te3 powder, as-deposited and annealed films shown in Fig. 1 1(a)-(d). The powder has a good crystalline nature with structure of Bi2Te3 that is rhombohedral with the space group (R3m)[21]. The grain size of initial powder was obtained between 14 -15 nm from XRD diffraction pattern. As can be seen as-prepared thin film with the thickness of 70 nm has a weak peak at 2θ equals to 40.61(Fig.2b), which corresponds to diffraction of (1 1 0) planes. After annealing process the Bi2Te3 thin films become polycrystalline as shown in Fig.2c. Sample annealed at 400 K has an additional peak at 2θ equals to 38.11 which corresponds to (1 0 10) plane. The results show that annealing change the polycrystalline with changing the preferential orientation of deposited Bi2Te3 thin films from (110) to (1010) plane. With increasing the annealing temperatures more peaks where observed (Fig. 2d). The (015),(1010), (110), (116), (2 1 1), (3 0 6) and (2 0 20) peaks were observed at 2? = 27.66, 38.2, 41.26, 44.39, 64.52, 77.47 and 81.62 respectively but these peaks have much lower intensity than the peak corresponding to the reflection to (1 0 10) plane. The lattice parameters of the films were calculated using the Bragg's formula

$$2d\sin\theta = n\lambda \tag{1}$$

where d is the plane spacing, θ is the diffraction angle and λ ($\lambda = 1.5406A^o$) is the radiation wavelength. The calculated lattice parameters were a=3.83 A^o and c=29.7 which are closed to the reported values for bulk, a=4.38 A^o and c=30.48 A^o [22,**?**,**?**]. The grain size (D) of the Bi2Te3 thin films annealed at various temperatures is estimated using Scherrer's formula:

$$D = \frac{k\lambda}{B\cos\theta} \tag{2}$$

where k is the constant=0.94, and B the full-width half-maximum. The grain size of the Bi2Te3 thin films of thickness 70 nm before and after annealing is shown in Table.1. The increase in the grain size may be attributed to the reorientation of the grain boundaries due to annealing According to this table one can deduce that with the increasing of the annealing temperature the crystallinity of the film is improved. These data indicate that at low annealing temperatures, the nano-particles exist in more strained form with the atomic entities in non-equilibrium positions, which relax to the equilibrium positions at higher temperature [25]. Another possible reason may be that the domain mobility is restricted due to pinning of the domain boundaries by crystal defects. The micro strain (ε) and the dislocation density (ρ) of the

as-grown and annealed films were calculated using the equations [26]:

$$\varepsilon = \frac{B\cos\theta}{4} \tag{3}$$

and

$$\rho = \frac{15\varepsilon}{aD}. \tag{4}$$

Table 1 suggests that the structural parameters of Bi2Te3 thin films are highly influenced by the annealing effect and with increasing annealing temperatures, the micro strain and dislocation density decrease. This may be due to the movement of interstitial Bi atoms from its grain boundary to the crystallites, which may be leading to reduction in the concentration of lattice imperfections [27].On the other hand, increasing grain size and decreasing micro strain and dislocation density indicated that homogeneous Bi2Te3 dispersion within the layers. Exactly this result will see in AFM images and AFM confirm them (Fig. 2.3).

Table 4: Variation of the band gap energy with annealed temperature

Thickness (nm)	Annealed. Temp. (°K)	Band gap energy (eV)
70	-----	3.650
	400	3.554
	420	3.500
	435	3.456
	450	3.410

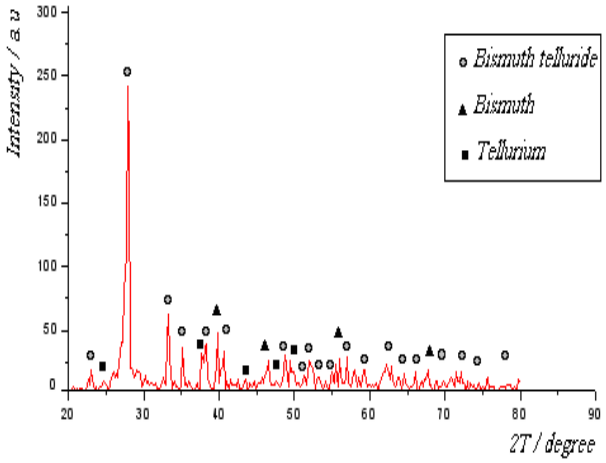

Fig. 1: X-Ray diffraction of powder Bi2Te3 film with thickness 70 nm

4.2 AFM studies

AFM has been used to see the top surface morphology of the thin films. It gives us information regarding the average size and distribution of the particles. AFM studies were performed by scanning probe microscope (Auto probe CP, Park Scientific) in ambient conditions. The scan was taken by 100 ? scanner using silicon nitride tip (radius of curvature 200) in a constant force (2 nN) contact mode. The 3D-AFM images corresponding to the as-deposited films with thickness of 37 and 110 nm and also those of 70 nm thin films annealed at 400 and 450 K were shown in Fig.3 It is observed that the surface morphology of Bi2Te3 thin films is significantly changed by changing annealing temperature and thickness. Fig. 3, Fig. 4 show us the development of morphology with increasing thickness. Thin films with d=37 nm exhibit randomly distributed grains, which changes into a idiomorphic grain growth in higher thickness and leads to grain coarsening in thick films (d=110 nm). Also as it can be seen in Fig.5 6 the film annealed in 450 K shows a coarsening compared with the other samples by lower annealing temperatures. The RMS roughness's which have been calculated from the height distribution and average roughnesses of the samples are shown in Table 2. It can be seen that annealing decreased sharply RMS roughness's of films that can be explained by diffusion effect in thin films and it causes layers have smoother surface after annealing.

Table 5: Variation of the band gap energy with thickness

Thickness (nm)		Band gap energy (eV)
58		3.755
70		3.650
84		2.800
110		2

4.3 Optical properties

Fig. **??**shows the optical absorption spectra of the films of thickness 58 and 70 nm. It is obvious that the absorption increases with increasing film thickness and it can be seen the Bi2Te3 films are having considerable absorption in the visible rang. The absorption coefficient (α) was calculated from absorption spectra with the help of the relation [28]:

$$\alpha = \frac{1}{t}(\ln(1/T)) \tag{5}$$

where t is the thickness of the film and T is transmittance. The optical absorption coefficient is nearly high for all the

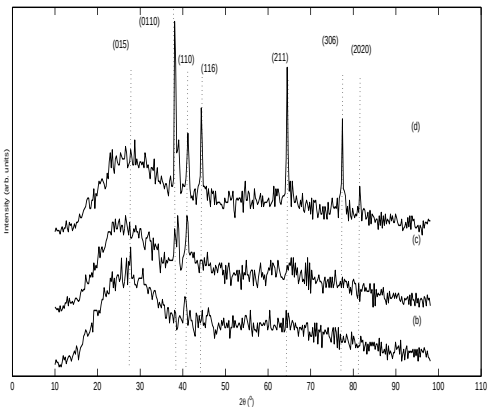

Fig. 2: X-Ray diffraction of (b) as-grown and (d), (c) annealed Bi2Te3 film of thickness 70 nm respectively in 400 and 450 K

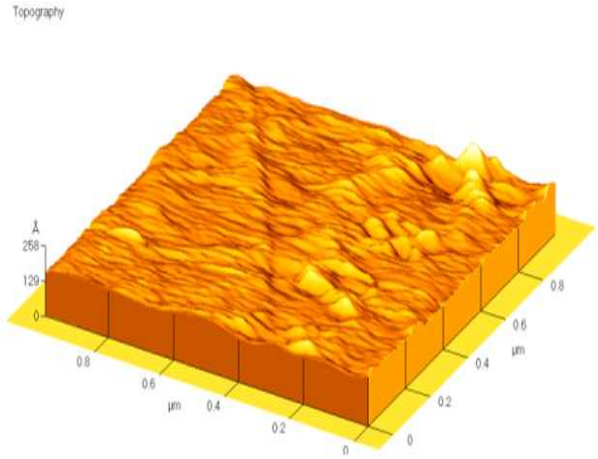

Fig. 3: 3D-AFM image of as-deposited films with thickness 37 nm

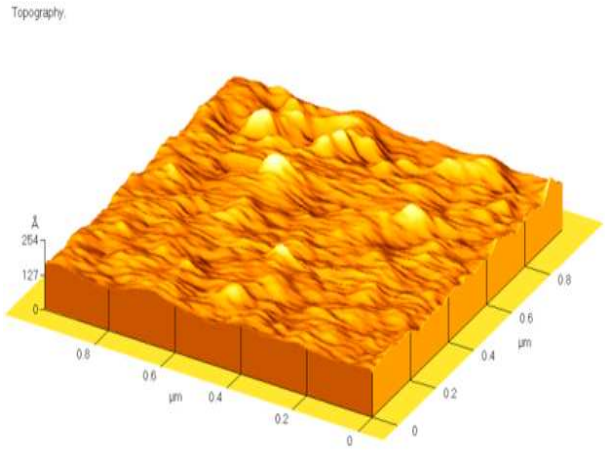

Fig. 4: 3D-AFM image of as-deposited films with thickness 110 nm

films with different thickness ($\alpha = 10^3$ cm^{-1}) (Table 3). The nature and value of the optical band gap, Eg, can be determined with the aid of the relation between absorption coefficient, α , and the incident photon energy, $h\nu$, as follows [29]:

$$\alpha h\nu = A(h\nu - E_g)^n \tag{6}$$

where A is constant and n assumes values of 1/2, 2, 3/2 and 3 for allowed direct, best optical absorption of Bi2Te3 thin films were obtained with n=1/2 as direct and allowed transitions. The optical gaps have been then determined by the extrapolation of the linear regions on energy axis. From the plots of $(\alpha h\nu)^2 versus h\nu$, the optical band gap energy has been estimated for different thickness and annealing temperatures . Fig.7(a, b) and Table 4, show that with the increase of film thickness the band gap energy decreases. This can be due to the increase of grain size with the increase of the film thickness [27]. Also from Fig.8 and Table 5, it is obvious that the optical band gap is a decreasing function of annealing temperature. Table 1 shows that with decreasing grain size the dislocation density increases. It has been suggested [30] that when the dislocation density is fairly high there is an increase in band gap of the semiconductor material because of the presence of dislocations provided that the dislocations are separated by a distance greater than the interatomic distance [31]. These results also supported by XRD studying as mentioned in section (3.1). On the other hand, it can be explained the decreasing of band gap with increasing thickness regarding that increasing the thickness causes to nanoparticles increased in which valance and conduction bands are wider and the gap between them is narrower.

5 Conclusion

Using sonochemical method to prepare Bi2Te3 nanoparticle with about 15 nm grain size, Bi2Te3 thin films were deposited on glass substrate by using thermally evaporated method. The influences of some preparation conditions, such as film thickness, annealing temperatures on structural, and optical properties of Bi2Te3 thin films have been studied. XRD studies indicate that annealed films are polycrystalline in structure with preferred orientation along (1 0 10). It was obvious that annealing improved crystallinity. The annealed film's lattice parameters are estimated as a=3.83 A^o and c=29.7 A^o. The grain size and the dislocation density of the material were found to be dependent on annealing and a significant increase in the grain size was also observed due to annealing. It was found that the

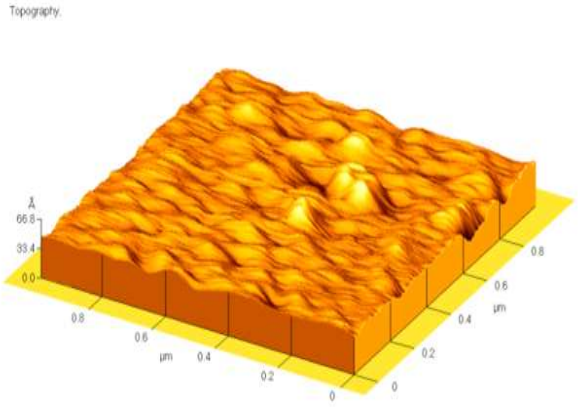

Fig. 5: 3D-AFM image of the film with thickness 70 nm annealed in 400 K

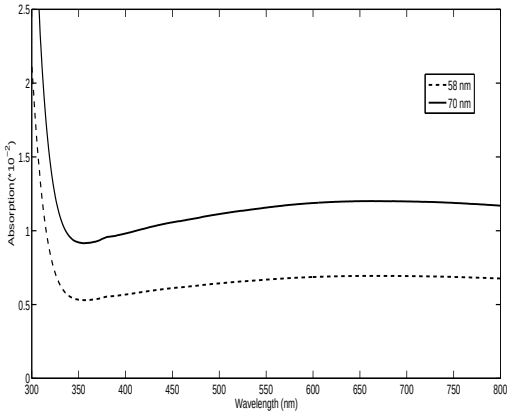

figurecaptionThe optical absorption spectra of the as-deposited films with 58 and 70 nm.

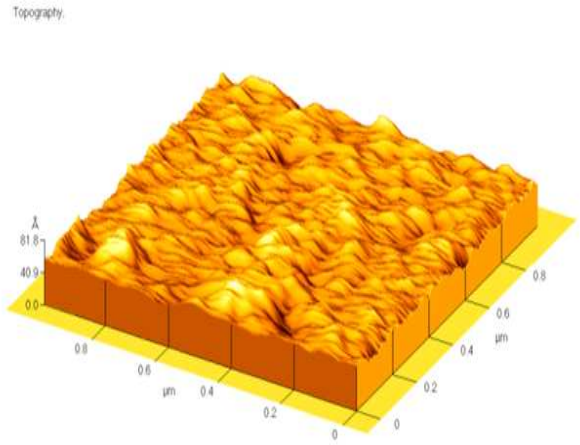

Fig. 6: 3D-AFM image of the film with 70 nm annealed in 450 K

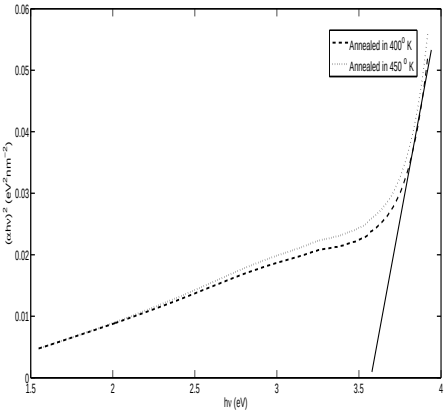

Fig. 7: The plot of $(\alpha h\nu)^2$ vs. $h\nu$ for films with thickness 70 nm annealed in 400 and 450 K.

RMS roughness increases by increasing thickness. The absorption coefficient and optical band gap were determined from the absorption spectra. The possible optical transition in these thin films is found to be direct and allowed. The energy band gap decreases as the film thickness and annealing temperature is increased.

References

[1] A. Aboulfarah, A. Mzerd, A. Giani, A. Boulouz, F. Pascal-Delannoy, A. Foucaran, A. Boyer, Mater. Chem. Phys., **62**, 179 (2000).
[2] B.B. Nayak, H.N. Acharya, T.K. Chaudhuri, G.B. Mitra, Thin Solid Films, **92**, 309 (1982).
[3] H. Wada, J. Morimoto, T. Miyakawa, T. Irie, Mater. Res. Bull., **26**, 179 (1991).
[4] I.-H. Kim, Mater. Lett. **44**, 75 (2000).
[5] A. Giani, F. Pascal-Delannoy, A. Boyer, A. Foucaran, M. Gschwind, P. Ancey, Thin Solid Films, **303**, 1 (1997).
[6] A. Giani, A. Boulouz, F. Pascal-Delannoy, A. Foucaran, A. Boyer, Thin Solid Films, **315**, 99 (1998) .
[7] E. Koukharenko , N. Frety , VG. Shepelevich , JC. Tedenac , J Alloys Compd., **299**, 254-7 (2000) .
[8] JY. Yang ,T. Aizawa ,A. Yamamoto,T. Ohta , J Alloys Compd., **312**, 326 (2000).
[9] XB. Zhao , XH. Ji , YH. Zhang , BH. Lu . J Alloys Compd., **368**, 349(2004).
[10] IJ. Ohsugi , T. Kojima , IA. Nishida . J Appl Phys., **68**, 5692 (1990).
[11] MM. Yim , FD. Rosi . Solid State Electron, **15**, 1121 (1972).
[12] Golis. Santosh,M. Arora , RK. Sharma , AC. Rastogi . Curr Appl Phys., **3**, 195 (2003).
[13] ZhouXi-Song, DengYuan,Nan Ce-Wen, LinYuan-Hua. J Alloys Compd., **352**, 328 (2003).

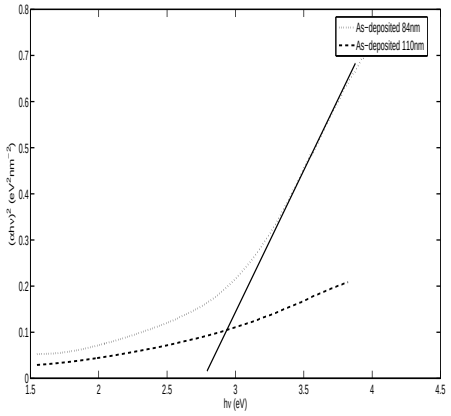

Fig. 8: The plot of $(\alpha h\nu)^2$ vs. $h\nu$ for as-deposited films 84 nm and 110 nm

[14] DM. Rowe , VS.Shukla , N. Savvides . J Cryst Growth, **1**, 542 (2001).
[15] JY. Yang , RG. Chen , XA. Fan , W. Zhu , SQ. Bao , XK. Duan .J Alloys Compd., **407**, 330 (2006).
[16] XA. Fan , JY. Yang , W. Zhu , RG. Chen , SQ. Bao , XK. Duan . J Alloys Compd., **420**, 256 (2006).
[17] J. Seo , K. Park , D. Lee , Lee. Mater Sci Eng B Solid-State Mater Adv Technol, **49**, 247 (1997).
[18] Seo J, Lee D, Lee C, Park K. J Mater Sci Lett., **16**, 1153 (1997).
[19] JY. Yang , W. Zhu , XH. Gao , SQ. Bao , XA. Fan . J Electroanal Chem., **577**, 117 (2005).
[20] W. Zhu, JY. Yang , J. Hou , XH. Gao , SQ. Bao , XA. Fan . J Electroanal Chem **585**,83 (2005).
[21] S.K.Mishra, S.Satpathy, O.Jepsen, Condens. Matter, **9**, 461 (1997).
[22] M.H. Francombe, Phil. Mag., **10**, 989 (1964).
[23] Sunglae Cho, Yunki Kim, Antonio DiVenere, George K. Wong, John B. Ketterson, Jerry R.Meyer, Appl. Phys. Lett., **75**, 1401 (1999).
[24] A. Giani, A. Boulouz, F. Pascal- Delannoy, A. Foucaran, A. Boyer, Thin SolidFilms, **315**, 99 (1998).
[25] S. Kongtaweelert ,D.C. Sinclair, S. Panichphant, Current Applied Physics, **6**, 474-477 (2006).
[26] C.K. De, N.K. Mishra, Indian J. Phys. A, **71**, 530 (1997) .
[27] J. Dheepa et al. J. Crystal Growth, **274**, 100 (2005).
[28] A. Goswami, Thin Film Fundamentals, New Age International Publishers, New Delhi, (1996).
[29] G. Sinha, K. Adhikary, S. Chaudhuri, J. Phys.: Condens. Matter., **18**, 2409 (2006).
[30] H.F. Matare, Defect Electronics in Semiconductors, Wiley, New York, (1971).
[31] S. Subramanian, D.P. Padiyan , Materials Chemistry and Physics, **107**, 392 (2008).